

Experimental demonstration of an analytic method for image reconstruction in optical diffusion tomography with large data sets

Zheng-Min Wang, George Y. Panasyuk, Vadim A. Markel, and John C. Schotland

Departments of Bioengineering and Radiology, University of Pennsylvania, Philadelphia, Pennsylvania 19104

Received August 12, 2005; accepted August 17, 2005

We report the first experimental test of an analytic image reconstruction algorithm for optical tomography with large data sets. Using a continuous-wave optical tomography system with 10^8 source–detector pairs, we demonstrate the reconstruction of an absorption image of a phantom consisting of a highly scattering medium containing absorbing inhomogeneities. © 2005 Optical Society of America

OCIS codes: 170.3880, 290.1990.

Optical diffusion tomography (ODT) is a biomedical imaging modality that utilizes diffuse light as a probe of tissue structure and function. Clinical applications include imaging of breast disease and functional neuroimaging. The physical problem that is considered is how to reconstruct the optical properties of an inhomogeneous medium from measurements taken on its surface. In a typical experiment, optical fibers are used for illumination and detection of the transmitted light.^{1–3} The number of measurements (source–detector pairs) that can be obtained, in practice, varies between 10^2 and 10^4 . A recently proposed alternative to fiber-based experiments is to employ a narrow incident beam for illumination. The beam can be scanned over the surface of the medium while a lens-coupled CCD detects the transmitted light. Using such a noncontact method makes it possible to avoid many of the technical difficulties that arise from fiber–sample interactions.^{4–6} In addition, extremely large data sets of approximately 10^8 – 10^{10} measurements can readily be obtained. Data sets of this size have the potential to vastly improve the quality of reconstructed images in ODT.^{7,8}

The reconstruction of images from large data sets is an extremely challenging problem owing to the high computational complexity of numerical approaches to the inverse problem in ODT. To address this challenge, we have developed analytic methods to solve the inverse problem.^{7–9} These methods lead to a dramatic reduction in computational complexity and have been applied in numerical simulations to data sets as large as 10^{10} measurements.⁷ In this Letter we report the first experimental demonstration of the feasibility of image reconstruction by using our analytic methods for optical tomography with large data sets. A noncontact ODT system with 10^8 source–detector pairs was employed to reconstruct the optical absorption of a highly scattering medium containing absorbing inhomogeneities.

We begin by considering the propagation of diffuse light in an absorbing medium. The density of electromagnetic energy $u(\mathbf{r})$ is assumed to satisfy the diffusion equation $-D\nabla^2 u(\mathbf{r}) + \alpha(\mathbf{r})u(\mathbf{r}) = S(\mathbf{r})$, where $\alpha(\mathbf{r})$ is the absorption coefficient, $S(\mathbf{r})$ is the power density

of a continuous wave source, and D is the diffusion constant. The energy density is taken to obey the boundary condition $u + \ell \hat{\mathbf{n}} \cdot \nabla u = 0$ on the surface bounding the medium, where $\hat{\mathbf{n}}$ is the unit outward normal and ℓ is the extrapolation length.¹⁰ The relative intensity measured by a point detector at \mathbf{r}_2 due to a point source at \mathbf{r}_1 is given, within the accuracy of the first Rytov approximation, by the integral equation

$$\phi(\mathbf{r}_1, \mathbf{r}_2) = \int d^3r G_0(\mathbf{r}_1, \mathbf{r}) G_0(\mathbf{r}, \mathbf{r}_2) \delta\alpha(\mathbf{r}), \quad (1)$$

where the source and detector are oriented in the inward and outward normal directions, respectively.⁸ Here $\delta\alpha(\mathbf{r}) = \alpha(\mathbf{r}) - \alpha_0$ denotes the spatial fluctuations in $\alpha(\mathbf{r})$ relative to a reference medium with absorption α_0 , G_0 is the Green's function for the diffusion equation with $\alpha = \alpha_0$, and the data function ϕ is defined by $\phi(\mathbf{r}_1, \mathbf{r}_2) = -G_0(\mathbf{r}_1, \mathbf{r}_2) \ln[I(\mathbf{r}_1, \mathbf{r}_2)/I_0(\mathbf{r}_1, \mathbf{r}_2)]$, where $I(\mathbf{r}_1, \mathbf{r}_2)$ denotes the intensity in the medium and $I_0(\mathbf{r}_1, \mathbf{r}_2)$ is the intensity in the reference medium. Note that the intensity is related to the Green's function by the expression $I(\mathbf{r}_1, \mathbf{r}_2) = cS_0(1 + \ell^*/\ell)^2/4\pi G(\mathbf{r}_1, \mathbf{r}_2)$, where S_0 is the source power and the transport mean free path ℓ^* is related to the diffusion coefficient by $D = 1/3c\ell^*$. We further note that the ratio of intensities in the definition of ϕ may be interpreted as a calibration step in an experiment.

We have constructed a noncontact ODT system to test the analytic method of image reconstruction. The source is a continuous-wave stabilized diode laser (DL7140-201, Thorlabs) operating at a wavelength of 785 nm with an output power of 70 mW. The laser output is divided into two beams by a beam splitter. The reflected beam is incident on a powermeter, which monitors the stability of the laser intensity. The transmitted beam passes through a lens onto a pair of galvanometer-controlled mirrors (SCA 750, Lasesys). The mirrors are used to scan the beam, which has a focal spot size of 200 μm , in a raster fashion over the surface of the sample. After propagating through the sample, the transmitted light passes through a bandpass interference filter

(10LF20-780, Newport) and is imaged onto a front illuminated thermoelectric-cooled 16 bit CCD array (DV435, Andor Technology) by a 23 mm/*f*1.4 lens. A mechanical shutter is placed in front of the CCD to reduce artifacts associated with frame transfer within the CCD chip. A pulse generator with digital delay is used to trigger and synchronize the CCD, the shutter, and the position of the beam.

The sample chamber is a rectangular box of depth 5 cm with square faces of area 50 cm × 50 cm constructed of clear acrylic sheets. The beam is scanned on one face of the sample, and the opposite face is imaged by the CCD. The chamber is placed equidistantly from the CCD and the laser source along the optical axis at a distance of 110 cm. The chamber is filled with a scattering medium, which consists of a suspension of 1% Intralipid in water in which absorbing objects may be suspended.

A tomographic data set is acquired by raster scanning the beam over a 29 × 29 square lattice with a lattice spacing of 0.5 cm. This yields 841 source positions within a 14 cm × 14 cm area centered on the optical axis. For each source, a 429 × 429 pixel region of interest is read out from the CCD. This results in 184,041 detectors arranged in a square lattice with an effective lattice spacing equivalent to 0.065 cm and all detectors located within a 28 cm × 28 cm area centered on the optical axis. Thus a data set of 1.5 × 10⁸ source–detector pairs is acquired.

The inverse problem in ODT consists of reconstructing $\delta\alpha$ from measurements of ϕ . In this Letter we consider the inversion of the integral equation (1) in the slab measurement geometry. The approach taken is to construct the singular value decomposition of the integral operator whose kernel is defined by Eq. (1) and to use this result to obtain the pseudo-inverse solution to Eq. (1). The starting point for this development is to consider the lattice Fourier transform of the sampled data function, which is defined by $\tilde{\phi}(\mathbf{q}_1, \mathbf{q}_2) = \sum_{\mathbf{r}_1, \mathbf{r}_2} \exp[i(\mathbf{q}_1 \cdot \mathbf{r}_1 + \mathbf{q}_2 \cdot \mathbf{r}_2)] \phi(\mathbf{r}_1, \mathbf{r}_2)$, where the sum is carried out over the square lattices of sources and detectors with lattice spacings h_s and h_d , respectively. The wave vectors \mathbf{q}_1 and \mathbf{q}_2 belong to the first Brillouin zones of the corresponding lattices, denoted FBZ(h_s) and FBZ(h_d). It can then be shown that the pseudoinverse solution to the integral equation (1) is given by the inversion formula

$$\delta\alpha(\mathbf{r}) = \int_{\text{FBZ}(h_s)} d^2q \int_{\text{FBZ}(h_d)} d^2p K(\mathbf{r}; \mathbf{q}, \mathbf{p}) \tilde{\phi}(\mathbf{q} - \mathbf{p}, \mathbf{p}), \quad (2)$$

where the kernel K is defined in Ref. 8. Several aspects of Eq. (2) are important to note. First, in the absence of noise, the transverse spatial resolution of reconstructed images is determined by the spatial frequency of sampling of the data function with respect to both source and detector coordinates. As a consequence, a large number of source–detector pairs are necessary to achieve the highest possible spatial resolution. It can be seen that when the source and detector lattices have equal spacing, the theoretical

limit of transverse resolution is given by the lattice spacing.⁷ When the source and detector lattice spacings are different, as is the case in the experiment reported here (where $h_s = 0.5$ cm and $h_d = 0.065$ cm), the resolution of reconstructed images is controlled by the larger lattice spacing.⁸ The overall spatial extent of the sources and detectors (windowing of the data function) is also known to strongly influence spatial resolution.⁷ Second, the inverse problem in ODT is overdetermined. In addition, it is highly ill posed. As a result, it can be said that large data sets allow the data function to be averaged in such a way that the sensitivity to noise in the inverse problem is partially ameliorated. Finally, inversion based on Eq. (2) is analytic in the sense that in certain geometries, such as the slab geometry employed in this study, the kernel K can be calculated explicitly.^{8,9}

The first step in the reconstruction of tomographic images is to measure the reference intensity I_0 for each source–detector pair. By fitting these data in the spatial frequency domain to the intensity I with $\alpha = \alpha_0$, we obtain the diffuse wavenumber $k_0 = \sqrt{\alpha_0/D} = 0.58$ cm⁻¹ and the extrapolation length $\ell = 0.7$ cm. Note that these parameters define the diffusion Green's function G in the slab geometry.¹⁰ Next, the object to be imaged is placed in the sample chamber, and the intensity I for each source–detector pair is measured. In Fig. 1 we show the reconstruction of a pair of black metal balls. The balls have a diameter of 8 mm and were suspended in the midplane of the

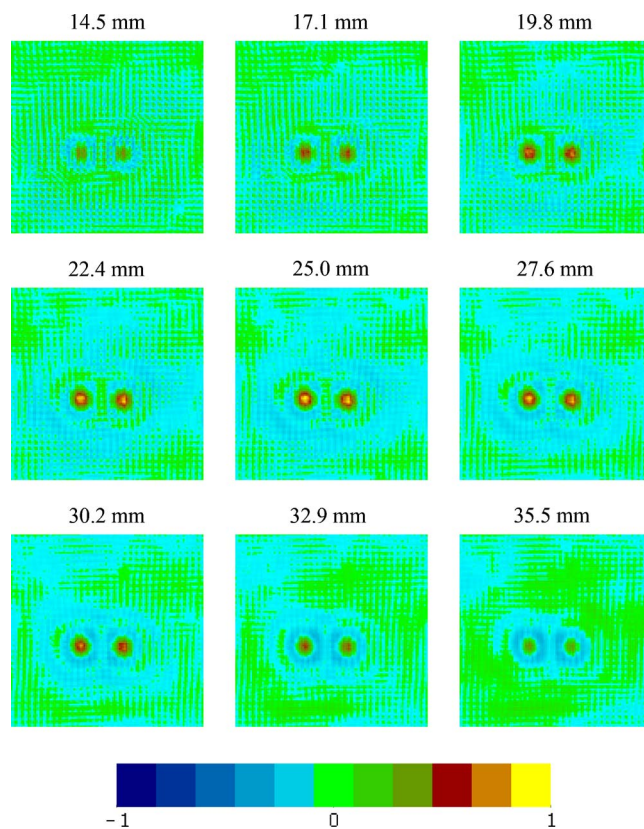


Fig. 1. (Color online) Reconstructions of $\delta\alpha$ for the two-ball phantom plotted on a linear color scale. The distance of each slice from the plane of sources is indicated. All images are normalized to the maximum of the central slice.

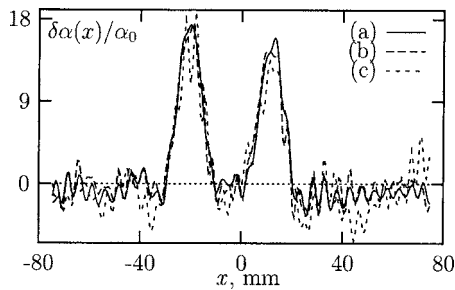


Fig. 2. One-dimensional profiles of the reconstructed absorption along the line passing through the centers of the balls in the central slice. Results for different values of the detector separation h_d are shown: (a) $h_d=0.65$ mm, (b) $h_d=5.2$ mm, (c) $h_d=10.4$ mm.

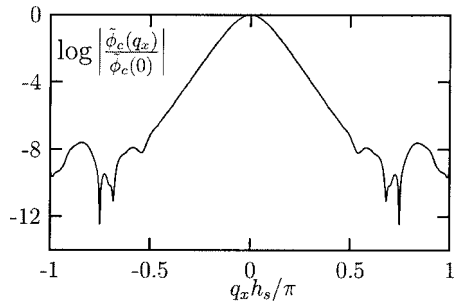


Fig. 3. Frequency components of the data function for the central source where $\tilde{\phi}_c(q_x) = \sum_{x,y} \exp(iq_x x) \phi(0,0;x,y)$ with the sum carried out over the lattice of detector positions.

sample chamber at a constant height with a separation of 3.2 cm. Tomographic images were reconstructed with a $15 \text{ cm} \times 15 \text{ cm}$ field of view by using 230×230 pixels per image with a separation between the slices of 0.26 cm. It can be seen in the central slice, which is equidistant from the source and the detector planes, that the balls are well resolved. The shallower and deeper slices show that the balls remain well resolved but with a smaller diameter, as expected. Figure 2 is a plot of $\delta\alpha/\alpha_0$ along the line passing through the centers of both balls in the central slice. The distance between the peaks is 3.3 cm, in close agreement with the measured separation of the balls. The FWHM of the peaks is 1.0 cm, which slightly overestimates the diameter of the balls.

Several comments on the above results are necessary. First, it can be seen that the resolution of reconstructed images is primarily controlled by the source separation h_s and is further limited by noise. To illustrate this point we have investigated the dependence of the reconstructed images on the detector spacing h_d . As is shown in Fig. 2, we find that the FWHM is extremely stable under decimation of the detector lattice until h_d approaches h_s , corresponding to 2.3×10^6 source–detector pairs. This result is consistent with numerical simulations of the reconstruction of

an ideal point absorber carried out under conditions identical to the experiment reported here. It is important to note that previously reported simulations⁷ indicate the potential for further improvement in resolution with decreasing h_s . However, for the experiment described in this Letter, there is significant onset of noise at a spatial frequency of approximately $1.5h_s^{-1}$, which precludes improvements in resolution at smaller source separations, as is illustrated in Fig. 3. Second, it is important to note that the reconstructed contrast in $\delta\alpha$ is not expected to be quantitative owing to the possible breakdown of the diffusion approximation in the interior of the strongly absorbing balls. Interestingly, however, the shape of the spherical absorbers is recovered well. Finally, the analytic method of image reconstruction is extremely efficient computationally and when applied to a data set consisting of 10^8 source–detector pairs requires about 10 min of CPU time on a 1.5 GHz workstation. It is important to note that reconstructions of data sets of this size are not feasible by using standard numerical reconstruction algorithms in ODT.⁸

In conclusion, we have demonstrated the feasibility of analytic methods for image reconstruction in ODT with large data sets. We are currently conducting further studies to assess the effects of absorption contrast on image resolution. We expect that with further technological advances and experimental refinements improvements in spatial resolution will be achieved.

This research was funded by the National Institutes of Health under grants P41RR02305 and R21EB004524. Support from the Whitaker Foundation is also gratefully acknowledged. J. C. Schotland's e-mail address is schotland@seas.upenn.edu.

References

1. F. Schmidt, M. Fry, E. Hillman, J. Hebden, and D. Delpy, *Rev. Sci. Instrum.* **71**, 256 (2000).
2. T. McBride, B. Pogue, S. Jiang, U. Osterberg, and K. Paulsen, *Rev. Sci. Instrum.* **72**, 1817 (2001).
3. S. Colak, M. van der Mark, G. Hooft, J. Hoogenraad, E. van der Linden, and F. Kuijpers, *IEEE J. Sel. Top. Quantum Electron.* **5**, 1143 (1999).
4. R. Schulz, J. Ripoll, and V. Ntziachristos, *Opt. Lett.* **28**, 1701 (2003).
5. G. Turner, G. Zacharakis, A. Soubret, J. Ripoll, and V. Ntziachristos, *Opt. Lett.* **30**, 409 (2005).
6. D. Cuccia, F. Bevilacqua, A. Durkin, and B. Tromberg, *Opt. Lett.* **30**, 1354 (2005).
7. V. A. Markel and J. C. Schotland, *Appl. Phys. Lett.* **81**, 1180 (2002).
8. V. A. Markel and J. C. Schotland, *Phys. Rev. E* **70**, 056616 (2004).
9. J. C. Schotland, *J. Opt. Soc. Am. A* **14**, 275 (1997).
10. V. Markel and J. Schotland, *J. Opt. Soc. Am. A* **19**, 558 (2002).